## IV. Numerical Examples for Continuous Malvar Wavelets

We take $a_{-1} = -5$, $a_0 = 0$, and $a_1 = 10$. There is one asymmetric overlap between $(a_{-1}, a_0]$ and $(a_0, a_1]$, which is $(-2, 4]$, i.e., $\epsilon_0^L = 2$ and $\epsilon_0^R = 4$. The local bases are

$$f_{j,k}(x) = \sqrt{\frac{2}{a_{j+1} - a_j}} \sin\left(\pi(k + 0.5)\frac{x - a_j}{a_{j+1} - a_j}\right)$$
$$k = 0, 1, 2, \cdots$$

The window function $\hat{w}_0(x)$ is the one in (2.3) shown in Fig. 1. The original test signal $s(t)$ is shown in Fig. 4(a). Figs. 2(a) and (b) show the lapped orthogonal transforms $\langle s, \tilde{f}_{j,k}\rangle_{L^2(\boldsymbol{R})}$, $k = 0, 1, \cdots, 40$ for $j = -1, 0$, respectively. Figs. 3(a) and (b) show the reconstructions of $s(t)$ from its LOT in Fig. 2 (a) and (b), respectively. Fig. 4(b) shows the whole reconstructions of $s(t)$ from its LOT in Fig. 2. The error between the true signal in Fig. 4(a) and its reconstruction by using the above asymmetric overlap in Fig. 4(b) is shown in Fig. 5(a). We also compute the reconstruction by using a symmetric overlap with $\epsilon_0^L = \epsilon_0^R = 2$. The error is shown in Fig. 5(b).

## V. Conclusions

In this correspondence, we have extended continuous-time Malvar wavelets with symmetric overlaps to the ones with asymmetric overlaps. We have shown that it is impossible to have discrete-time Malvar wavelets with asymmetric overlaps unless the overlaps become symmetric. Numerical examples for continuous-time Malvar wavelets were presented to illustrate the theory.

## References


[1] H. S. Malvar, "Lapped transforms for efficient transform/subband coding," *IEEE Trans. Signal Processing*, vol. 38, pp. 969–978, June 1990.

[2] ——, *Signal Processing with Lapped Transforms.* Norwood, MA: Artech, 1992.

[3] R. Coifman and Y. Meyer, "Remarques sur l'analyse de Fourier à fenètre," *C.R. Acad. Sci. Paris*, t.312, Serie I, pp. 259–261, 1991.

[4] B. W. Suter and M. E. Oxley, "On variable overlapped windows and weighted orthonormal bases, " *IEEE Trans. Signal Processing*, pp. 1973–1982, Aug. 1994.

[5] ——, "Getting around the Balian-Low theorem using generalized Malvar wavelets," in *Wavelets: Theory, Algorithm and Applications*, C. Chui *et al.*, Eds. San Diego, CA: Academic, 1994, pp. 295–310.

[6] M. V. Wickerhauser, "Smooth localized orthonormal bases," *C. R. Acad. Sci. Paris*, t.316, serie I, pp. 423–427, 1993.

[7] R. R. Coifman and M. V. Wickerhauser, "Entropy-based algorithms for best basis selection," *IEEE Trans. Inform. Theory*, vol. 38, pp. 713–718, Mar. 1992.

[8] X. G. Xia and B. W. Suter, "A systematic method for the construction of time-varying FIR multirate filter banks with perfect reconstruction," preprint, 1994.; also, in *TFTS Proc.*, 1994.

[9] Y. Meyer, *Wavelets: Algorithms and Applications.* Philadelphia, PA: SIAM, 1993.

[10] K. Nayebi, T. P. Barnwell and M. J. T. Smith, "Analysis-synthesis systems with time-varying filter bank structures," in *Proc. IEEE Int. Conf. Acoust., Speech, Signal Processing*, San Francisco, CA, Mar. 1992, vol. 4, pp. 617–620.

[11] I. Sodagar *et al.*, "A class of time-varying wavelet transforms," in *Proc. IEEE Int. Conf. Acoust., Speech, Signal Processing*, Minneapolis, MN, Apr. 1993, vol. 3, pp. 201–204.

[12] R. A. Gopinath and C. S. Burrus, "Factorization approach to unitary time-varying filter banks," Computational Math. Lab., Rice Univ., Houston, TX, Tech. Rep. CML TR92-23, Dec. 1992.

[13] C. Herley, J. Kovačević *et al.*, "Tilings of the time-frequency plane: construction of arbitrary orthogonal bases and fast tiling algorithms," *IEEE Trans. Signal Processing*, vol. 41, pp. 3341–3359, Dec. 1993.

[14] R. L. de Queiroz and K. R. Rao, "Time-varying lapped transforms and wavelet packets," *IEEE Trans. Signal Processing*, vol. 41, pp. 3293–3305, Dec. 1993.

[15] P. Auscher *et al.*, Local sine and cosine basis of Coifman and Meyer and the construction of smooth wavelets," in *Wavelets: A Tutorial in Theory and Applications*, C.K. Chui, Ed. Boston, MA: Academic, 1992, pp. 237–256.


# Wavelet Synthesis by Alternating Projections

J.-C. Pesquet and P. L. Combettes

***Abstract*—The coefficients of the quadrature mirror filters involved in orthonormal wavelet or wavelet packets signal decompositions are often chosen in an *ad hoc* manner. In order to adapt such a decomposition to the signal being analyzed, it may be pertinent to maximize an energy concentration criterion, which leads to a constrained optimization problem. In this correspondence, a simple geometric interpretation of this problem is given, and an alternating projection method is proposed to solve it.**

## I. Introduction

A central problem in wavelet $L^2$-signal analysis is to determine a basis in order to best extract pertinent information. One approach is to select the structure of the filter bank that is optimal in terms of a preset criterion, e.g., entropy [7]. An alternative approach, and the one we adopt here, is to optimize the coefficients of the filter involved in a given filter bank structure [20], [22]. The resulting constrained optimization problem can be posed in terms of the paraunitary quadrature mirror filters (QMF's) that arise in the implementation of wavelet decompositions [27] (cf. Fig. 1). Let us assume that the underlying orthogonal filters have real and finite impulse responses (FIR's) $(h_k)_{k\in\mathbb{Z}}$ and $(g_k)_{k\in\mathbb{Z}}$, say

$$(\forall k \in \mathbb{Z})\ h_k = g_k = 0, \quad \text{if} \quad k < 0 \quad \text{or} \quad k \geq L \tag{1}$$

(where $L$ is necessarily even [10]). Thanks to the realness of the sequences, we can restrict the spectral domain to $[0, \pi]$, and the orthonormality of the resulting basis then translates into the constraint

$$(\forall \omega \in [0, \pi])\ |G(e^{i\omega})|^2 + |G(-e^{i\omega})|^2 = 2 \tag{2}$$

where $G$ is the $z$-transform of $(g_k)_{k\in\mathbb{Z}}$. It is recalled that the $z$-transform of $(h_k)_{k\in\mathbb{Z}}$ can be chosen as $H(z) = z^{1-L}G(-z^{-1})$. On the other hand, to obtain a regular wavelet basis [19], one can set

Manuscript received July 16, 1994; revised August 30, 1995. This work was supported in part by the National Science Foundation under Grant MIP-9308609. The associate editor coordinating the review of this paper and approving it for publication was Dr. Truong Q. Nguyen.

J.-C. Pesquet is with the Laboratoire des Signaux et Systèmes, CNRS/Université de Paris-Sud and GDR TdSI, Ecole Supérieure d'Electricité, Gif sur Yvette, France.

P. L. Combettes is with the Department of Electrical Engineering, City College and Graduate School, City University of New York, New York, NY 10031 USA.

Publisher Item Identifier S 1053-587X(96)02407-3.

1053–587X/96$05.00 © 1996 IEEE

Authorized licensed use limited to: N.C. State University Libraries - Acquisitions & Discovery S. Downloaded on November 01,2026 at 19:48:41 UTC from IEEE Xplore. Restrictions apply.

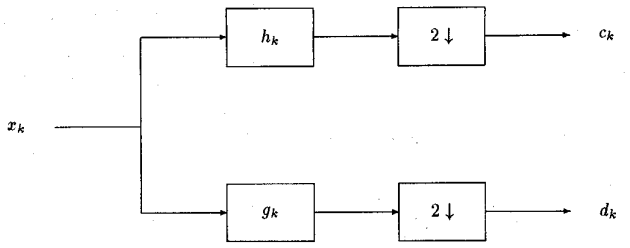



Fig. 1. Two-channel filter bank.

the first $N \leq L/2$ moments of $(g_k)_{k\in\mathbb{Z}}$ to zero. This constraint can be expressed as [10]

$$(\forall \omega \in [0,\pi])\ G(e^{i\omega}) = (1-e^{i\omega})^N G_1(e^{i\omega}) \tag{3}$$

where $G_1(z)$ is a polynomial of degree $L-N-1$ in $z^{-1}$. A common objective in signal analysis is to concentrate the energy of the signal on a few components of the decomposition. In the context of wavelet analysis, it has proven useful to concentrate the energy on the approximation coefficients $(c_k)_{k\in\mathbb{Z}}$ [2], [3], [11], [12], [16]–[18], [23]–[25]. This amounts to minimizing the energy of the detail coefficients $(d_k)_{k\in\mathbb{Z}}$, i.e.

$$E = \mathrm{E} \mid d_k \mid^2 = \frac{1}{2\pi}\int_{-\pi}^{\pi} |G(e^{i\omega})|^2 S(e^{i\omega}) d\omega \tag{4}$$

where the input signal $(x_k)_{k\in\mathbb{Z}}$ is assumed random and wide-sense stationary or deterministic and square summable with spectral density $S$. The operator E denotes, therefore, either mathematical expectation or summation over all integers $k$. Given the above constraints, the problem can be stated as

$$\text{Minimize } E \text{ in (4) subject to (1), (2), and (3).} \tag{5}$$

The goal of this correspondence is to present a simple iterative scheme to solve (5). Relevant work in this direction includes [23]–[25], where it was shown that the minimization of $E$ in (4) subject to (2) can be obtained by principal components analysis in the frequency domain[1] and gives

$$(\forall \omega \in [0,\pi])\ |G(e^{i\omega})| = \begin{cases} \sqrt{2} & \text{if } S(e^{i\omega}) \leq S(-e^{i\omega}), \\ 1/\sqrt{2} & \text{if } \omega = \pi/2, \\ 0 & \text{otherwise.} \end{cases} \tag{6}$$

Unfortunately, the filter thus obtained is not realizable. A great deal of effort has also been devoted to the problem of finding filters that minimize $E$ or another criterion under (1) and (2). These studies have resulted in a number of algorithms that are not guaranteed to provide globally optimal solutions [2], [3], [11], [12], [14]–[18], [24], [26].

In the following section, we interpret the basic problem (5) in geometrical terms. In this framework, it is simply reformulated as the problem of finding a point in a convex set that lies at minimum distance from an affine subspace. In Section III, we propose an alternating projection algorithm to solve this problem, and we establish its convergence to a globally optimal solution of (5). Finally, in the last section, we present an application of the method to the construction of a signal-adapted multiresolution analysis structure.

## II. Geometrical Formulation

In mathematical programming, convex constraints are easier to handle than nonconvex ones. In this regard, let us observe that in the Hilbert space $\ell^2$ of square-summable real sequences, the orthonormality constraint (2) is associated with a nonconvex set. Let us also note that if $(g_k)_{k\in\mathbb{Z}}$ is the impulse response of an FIR QMF filter that minimizes $E$, any other filter obtained through the spectral factorization of $P(z) = G(z)G(z^{-1})$ is also a solution to the problem. Therefore, it appears preferable to solve (5) in the space of sequences whose $z$-transform is $P$. The constraints (1)–(3) then become, for every $\omega$ in $[0,\pi]$

$$\begin{cases} P(e^{i\omega}) = 1 + \sum_{k=0}^{L/2-1} p_k \cos((2k+1)\omega), \\ P(e^{i\omega}) = (1-\cos\omega)^N Q(e^{i\omega}) \end{cases} \tag{7}$$

where

$$Q(e^{i\omega}) = \sum_{k=0}^{L-N-1} q_k \cos(k\omega) \tag{8}$$

and

$$Q(e^{i\omega}) \geq 0. \tag{9}$$

It is worth remarking that we can also write

$$\begin{cases} P(e^{i\omega}) = 1 + \sum_{k=0}^{L/2-1} p'_k (\cos\omega)^{2k+1}, \\ Q(e^{i\omega}) = \sum_{k=0}^{L-N-1} q'_k (\cos\omega)^k \end{cases} \tag{10}$$

where

$$\begin{cases} \mathbf{p} = [p_0, \cdots, p_{L/2-1}]^T = \mathbf{A}_1 [p'_0, \cdots, p'_{L/2-1}]^T, \\ \mathbf{q} = [q_0, \cdots, q_{L-N-1}]^T = \mathbf{A} [q'_0, \cdots, q'_{L-N-1}]^T. \end{cases} \tag{11}$$

The computation of the matrices $\mathbf{A}_1$ and $\mathbf{A}$ is straightforward and does not need to be included here. Since the problem can be conveniently formulated in terms of the vector $\mathbf{q}$, we shall henceforth place ourselves in the space $\mathbb{R}^{L-N}$. First, we need to rewrite the constraints (7) and (8) in this space. Substituting (10) and (11) into (7) yields

$$\begin{aligned} 1 + \sum_{k=0}^{L/2-1} p'_k (\cos\omega)^{2k+1} &= (1-\cos\omega)^N \sum_{k=0}^{L-N-1} q'_k (\cos\omega)^k \\ &= \sum_{m=0}^{N} \sum_{k=0}^{L-N-1} (-1)^m C_m^N [\mathbf{A}^{-1}\mathbf{q}]_k (\cos\omega)^{k+m} \end{aligned} \tag{12}$$

where $C_m^N = N!/(m!(N-m)!)$. Let $\mathbf{M}$ be the $L \times (L-N)$ Toeplitz matrix whose first column and row are $[C_0^N, -C_1^N, \cdots, (-1)^N C_N^N, 0, \cdots, 0]^T$, and $[C_0^N, 0, \cdots, 0]$, respectively, and let $\mathbf{M}_0$ (respectively, $\mathbf{M}_1$) be the matrix whose rows are the odd-numbered (respectively, even-numbered) rows of $\mathbf{M}$. Then, the coefficients of even powers of $\cos\omega$ in (12) give $L/2$ equations with $L-N$ unknowns $q_k$.[2] This means that the orthonormality condition

[1] This solution also ensures that the sequences $(c_k)_{k\in\mathbb{Z}}$ and $(d_k)_{k\in\mathbb{Z}}$ are uncorrelated.

[2] Note that (12) carries the implicit restriction that $L-N \geq L/2$, i.e., $N \leq L/2$.

Authorized licensed use limited to: N.C. State University Libraries - Acquisitions & Discovery S. Downloaded on November 01,2026 at 19:48:41 UTC from IEEE Xplore. Restrictions apply.

confines the vector $\mathbf{q}$ to the affine subspace $\mathcal{F}$ defined by

$$\mathcal{F} = \{\mathbf{q} \in \mathbb{R}^{L-N} \mid \mathbf{M}_0\mathbf{A}^{-1}\mathbf{q} = [1, 0, \cdots, 0]^T\}. \quad (13)$$

Similarly, the coefficients of odd powers in (12) give $L/2$ equations in $L/2$ unknowns $p'_k$, i.e.

$$\mathbf{p}' = [p'_0, \cdots, p'_{L/2-1}]^T = \mathbf{M}_1\mathbf{A}^{-1}\mathbf{q}. \quad (14)$$

Next, we observe that in the space $\mathcal{F}$, the nonnegativity constraint (9) is associated with the closed and convex set

$$\mathcal{S} = \bigcap_{\omega\in[0,\pi]} \{\mathbf{q} \in \mathcal{F} \mid \mathbf{f}(\omega)^T\mathbf{q} \geq 0\} \quad (15)$$

where $(\forall \omega \in [0, \pi])\ \mathbf{f}(\omega) = [1, \cos\omega, \cdots, \cos((L-N-1)\omega)]^T$. Note that membership in $\mathcal{S}$ can be tested by checking the sign of the polynomial form $\sum_{k=0}^{L-N-1} q'_k x^k$ for $x \in [-1, 1]$: If $\cos\omega_2$ and $\cos\omega_1$ are two consecutive roots of this polynomial such that $\omega_1 < \omega_2$, it is sufficient to evaluate

$$\int_{\omega_1}^{\omega_2} Q(e^{i\omega})\, d\omega = q_0(\omega_2 - \omega_1) + \sum_{k=1}^{L-N-1} \frac{q_k}{k}(\sin(k\omega_2) - \sin(k\omega_1)) \quad (16)$$

to check the sign of $Q(e^{i\omega})$ on $]\omega_1, \omega_2[$.

Let us now turn our attention to the geometrical formulation of the problem in $\mathcal{F}$. By writing $S(e^{i\omega})$ in the form $s_0 + 2\sum_{k=1}^{+\infty} s_k \cos(k\omega)$, where $(s_k)_{k\in\mathbb{Z}}$ represents the autocorrelation of the signal, the cost function (4) can be written as $E = (2\pi)^{-1}|\int_{-\pi}^{\pi} S(e^{i\omega})P(e^{i\omega})\, d\omega|$. Hence, by virtue of Parseval's equality, we obtain $E = |s_0 + \mathbf{s}^T\mathbf{p}|$, where $\mathbf{s} = [s_1, s_3, \cdots, s_{L-1}]^T$. According to (10) and (14), we have $E = |s_0 + \mathbf{b}^T\mathbf{q}|$, where $\mathbf{b}^T = \mathbf{s}^T\mathbf{A}_1\mathbf{M}_1\mathbf{A}^{-1}$. Denote by $\mathcal{D}$ the affine hyperplane in $\mathcal{F}$ such that

$$\mathcal{D} = \{\mathbf{q} \in \mathcal{F} \mid s_0 + \mathbf{b}^T\mathbf{q} = 0\}. \quad (17)$$

Then, $E = \|\mathbf{b}\|\, d(\mathbf{q}, \mathcal{D})$, where $d(\mathbf{q}, \mathcal{D}) = \inf\{\|\mathbf{q} - \mathbf{r}\| \mid \mathbf{r} \in \mathcal{D}\}$ is the distance between $\mathbf{q}$ and $\mathcal{D}$. In short, (5) can be recast in the finite-dimensional affine space $\mathcal{F}$ as the problem of finding a point $\mathbf{q}^*$ in a closed convex subset $\mathcal{S}$ that lies at minimum distance from the affine subspace $\mathcal{D}$.

## III. Numerical Solution

We have just seen that the basic problem (5) is equivalent to

$$\text{Find } \mathbf{q}^* \in \mathcal{G} = \{\mathbf{q} \in \mathcal{S} \mid d(\mathbf{q}, \mathcal{D}) = d(\mathcal{S}, \mathcal{D})\} \quad (18)$$

where $d(\mathcal{S}, \mathcal{D}) = \inf\{d(\mathbf{q}, \mathcal{D}) \mid \mathbf{q} \in \mathcal{S}\}$. We propose a method of alternating projections to solve this problem.[3]

### A. Algorithm

1) Choose $\mathbf{r}_0 \in \mathcal{D}$, $\eta \in ]0, +\infty[$, and $\varepsilon \in ]0, 1[$.
2) Set $n = 0$ and $\mathbf{q}_0 = P_{\mathcal{S}}(\mathbf{r}_0)$.
3) Choose $\lambda_n \in [\varepsilon, 2 - \varepsilon]$.
4) Set $\mathbf{r}_{n+1} = \mathbf{r}_n + \lambda_n(P_{\mathcal{D}}(\mathbf{q}_n) - \mathbf{r}_n)$.
5) Set $\mathbf{q}_{n+1} = P_{\mathcal{S}}(\mathbf{r}_{n+1})$.
6) If $\|\mathbf{q}_{n+1} - \mathbf{q}_n\| \geq \eta$, set $n = n + 1$ and return to 3).
7) Stop.

[3] Recall that if $\mathcal{C}$ is a nonempty closed and convex subset of a Hilbert space $\Xi$ with distance $d$, then for every point $\mathbf{q} \in \Xi$, there exists a unique point $P_{\mathcal{C}}(\mathbf{q}) \in \mathcal{C}$ such that $d(\mathbf{q}, P_{\mathcal{C}}(\mathbf{q})) = d(\mathbf{q}, \mathcal{C})$. $P_{\mathcal{C}}(\mathbf{q})$ is the projection of $\mathbf{q}$ onto $\mathcal{C}$.

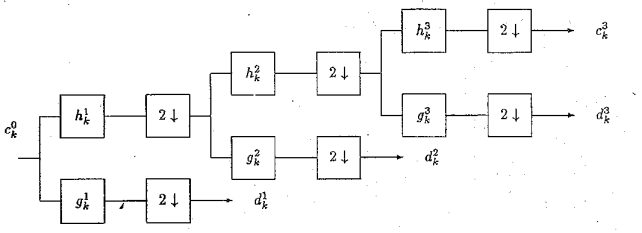



Fig. 2. Three-level multiresolution analysis structure.

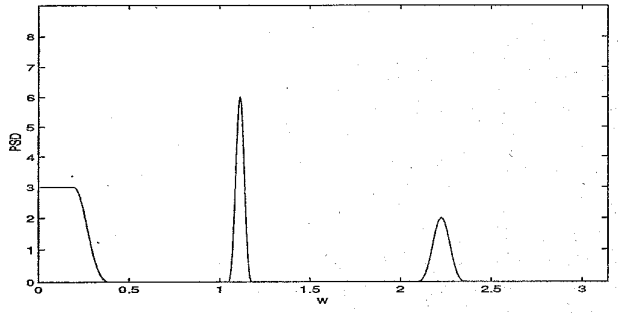



Fig. 3. Spectral density of the analyzed stationary random process.

### B. Convergence

The convergence of any sequence $(\mathbf{q}_n)_{n\in\mathbb{N}}$ generated by this algorithm to a point in $\mathcal{G}$ follows from the following argument. Since $P(e^{i\omega}) \geq 0$, Property (7) implies that $|p_k| \leq 2$, and therefore, $\|\mathbf{p}\| \leq \sqrt{2L}$. Moreover, one can check that according to (11), there exists $\alpha \geq 0$ such that $\|\mathbf{q}\| \leq \alpha\|\mathbf{p}\|$. This means that $\mathcal{S}$ is bounded and [9, Theorem 1] implies that for any initial conditions, the sequence $(\mathbf{r}_n)_{n\in\mathbb{N}}$ converges in $\mathcal{D}$ to a point $\mathbf{r}^* \in \mathcal{G}' = \{\mathbf{r} \in \mathcal{D} \mid d(\mathbf{r}, \mathcal{S}) = d(\mathcal{D}, \mathcal{S})\}$. Finally, the continuity of $P_{\mathcal{S}}$ in (5) guarantees that $(\mathbf{q}_n)_{n\in\mathbb{N}}$ converges to $P_{\mathcal{S}}(\mathbf{r}^*) \in \mathcal{G}$.

### C. Relaxations

The relaxation coefficients $(\lambda_n)_{n\in\mathbb{N}}$ can be varied at each iteration of the algorithm. It is shown in [9] that overrelaxations, i.e., $(\forall n \in \mathbb{N})$ $\lambda_n \in [1, 2 - \varepsilon]$, accelerate convergence toward a solution in our case; in addition, they can be adapted at each step to optimize the progression of the algorithm. Finally, let us note that in the unrelaxed case, i.e., $(\forall n \in \mathbb{N})\ \lambda_n = 1$, the proposed algorithm reduces to the standard projection algorithm $(\forall n \in \mathbb{N})\ \mathbf{q}_{n+1} = P_{\mathcal{S}}(P_{\mathcal{D}}(\mathbf{q}_n))$, whose convergence was established in [4].

### D. Computation of the Projections

The implementation of the algorithm requires the computation of projections onto $\mathcal{D}$ and $\mathcal{S}$ at each iteration. The projection onto $\mathcal{D}$ is easily obtained since $\mathcal{D}$ an affine hyperplane. The projection onto $\mathcal{S}$ is more complex, but it can be approximated by projecting onto the outer polyhedron $\mathcal{S}_M = \bigcap_{k=1}^{M} \{\mathbf{q} \in \mathcal{F} \mid \mathbf{f}(\omega_k)^T\mathbf{q} \geq 0\}$, where $\omega_k = (k-1)\pi/(M-1)$. This projection can be computed via the method proposed in [13], and the resulting projection error can be made arbitrarily small by making $M$ sufficiently large. Note that this kind of approximation is also used in [1]. In our case, the level of approximation that is required can be controlled thanks to (16), through which membership in $\mathcal{S}$ can be rigorously tested. However, a tight approximation is not required until convergence.

### E. Determination of the Impulse Responses

Once the optimal $\mathbf{q}^*$ has been determined by the alternating projections algorithm, the function $G_1$ in (3) can be obtained via a spectral factorization of $Q$; $(g_k)_{k\in\mathbb{Z}}$ is then deduced from $G_1$. Efficient

Authorized licensed use limited to: N.C. State University Libraries - Acquisitions & Discovery S. Downloaded on November 01,2026 at 19:48:41 UTC from IEEE Xplore. Restrictions apply.

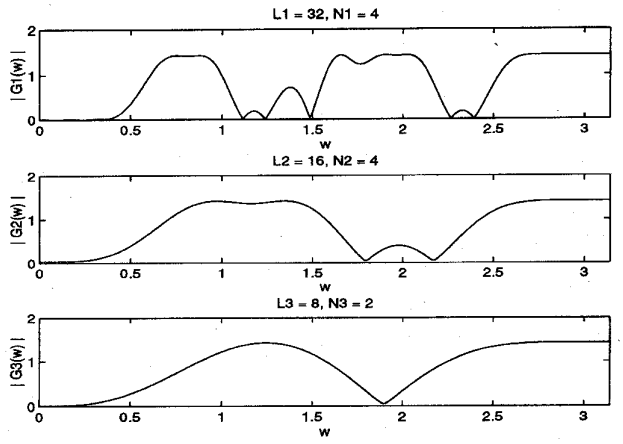



Fig. 4. Frequency responses of the optimized filters.

TABLE I
COMPARED PERFORMANCES OF OPTIMIZED AND STANDARD FILTERS

| | Optimal | Daubechies | Battle-Lemarié |
|---|---|---|---|
| $\text{NMSE}_1$ | 0.0196 | 0.1675 | 0.1683 |
| $\text{NMSE}_2$ | 0.0527 | 0.4139 | 0.4078 |
| $\text{NMSE}_3$ | 0.3270 | 0.4266 | 0.4281 |

spectral factorization algorithms can be found in the literature [16], [27]. In our experiments, we chose a cepstral method combined with a few iterations of a quasi-Newton method.

## IV. Signal-Adapted Multiresolution Analysis

We now consider an application of the proposed method to the multiresolution analysis of a signal $(x_k)_{k\in\mathbb{Z}} = (c_k^0)_{k\in\mathbb{Z}}$ decomposed by a wavelet-like hierarchical filter bank, as illustrated in Fig. 2. We add here a degree of freedom by allowing the use of different filters at each resolution level. This means that the resulting decomposition is not generally a standard orthonormal wavelet transform. However, as was shown in [5] and [6], a wider class of orthogonal transforms is thus obtained. This approach is also easier to handle since imposing the same filters at each resolution would introduce an additional constraint in the optimization problem. Specifically, we adopt a fine-to-coarse recursive strategy by starting the optimization at the highest available resolution ($j = 0$) and stopping the process at the lowest one ($j = j_m$). For $j = 1, \cdots, j_m$, the impulse responses $(h_k^j, g_k^j)_{k\in\mathbb{Z}}$ of the paraunitary QMF filters are determined by minimizing $\mathrm{E}|d_k^j|^2$ from the knowledge of the second-order attributes of $(c_k^{j-1})_{k\in\mathbb{Z}}$. Note that the merits of this kind of progressive optimization have also been recognized in [21] for the design of filter banks with improved time-frequency localizations.

In our example, a zero-mean stationary random process with the spectral density depicted in Fig. 3 is considered. Three levels of decomposition are performed ($j_m = 3$), and filters with lengths and numbers of vanishing moments $(L_j, N_j)$,, respectively, equal to (32, 4), (16, 4), and (8, 2) are used at resolution levels $j = 1$, 2, and 3. In our simulations, the algorithm typically converged in less than 220 iterations. Fig. 4 shows the frequency responses of $(g_k^j)_{k\in\mathbb{Z}}$. For the same lengths, these filters are compared to Daubechies' [10] in terms of energy compaction in Table I. The improvement is evaluated by calculating the normalized mean square error defined as $\text{NMSE}_j = \sum_{l=1}^{j} 2^{-l}\mathrm{E}|d_k^l|^2/\mathrm{E}|x_k|^2$. With the proposed method, $\text{NMSE}_j$ drops below 6% for $j \leq 2$, whereas, even for $j = 1$, it is above 15% for Daubechies' filters. Similar conclusions can be drawn from a comparison with Battle-Lemarié's [10] filters as illustrated in Table I. Battle-Lemarié's filters are chosen with the same number of vanishing moments as the optimized ones and their impulse responses have been truncated to the same length. It has been checked experimentally that the overall truncation error is negligible.

## V. Conclusion

The design of wavelet filters for signal analysis based on an energy concentration criterion has been formulated in a geometrical framework. A simple iterative technique has been proposed to obtain the globally optimal solution to this problem. The method is quite flexible and can be extended to incorporate other pertinent convex constraints. In this case, the algorithm remains the same, except that $\mathcal{S}$ is now the intersection of all the convex sets associated with the constraints. The projection onto $\mathcal{S}$ can be obtained via decomposition with respect to the individual sets, as discussed in [8]. The proposed approach is also applicable to other filter bank structures that may be more appropriate in certain problems.

## References

[1] J. A. Cadzow and Y. Sun, "Sequences with positive semidefinite Fourier transforms," *IEEE Trans. Acoust., Speech, Signal Processing*, vol. 34, no. 6, pp. 1502–1510, Dec. 1986.

[2] H. Caglar, Y. Liu, and A. N. Akansu, "Statistically optimized PR-QMF design," in *Proc. SPIE, Visual Commun. Image Processing*, vol. 1605, Nov. 1991, pp. 86–94.

[3] H. Caglar, B. Sankur, and E. Anarim, "Matched wavelet design and coding gain performance," in *Proc. Eighth IEEE Workshop Image Multidim. Signal Processing*, Cannes, France, Sept. 8–10, 1993, pp. 144–145.

[4] W. Cheney and A. A. Goldstein, "Proximity maps for convex sets," *Proc. Amer. Math. Soc.*, vol. 10, no. 3, pp. 448–450, June 1959.

[5] A. Cohen, "Non-stationary multiscale analysis," in *Wavelets, Theory, Algorithms and Applications*, C. K. Chui, L. Montefusco, and L. Puccio, Eds. San Diego, CA: Academic, 1994.

[6] A. Cohen and E. Séré, *Time-Frequency Localization with Nonstationary Wavelet Packets*, CEREMADE, Université Paris IX Dauphine, preprint, 1994.

[7] R. R. Coifman and M. V. Wickerhauser, "Entropy-based algorithms for best basis selection," *IEEE Trans. Inform. Theory*, vol. 38, no. 2, pp. 713–718, Mar. 1992.

[8] P. L. Combettes, "Signal recovery by best feasible approximation," *IEEE Trans. Image Processing*, vol. 2, no. 2, pp. 269–271, Apr. 1993.

[9] ——, "Inconsistent signal feasibility problems: Least-squares solutions in a product space," *IEEE Trans. Signal Processing*, vol. 42, no. 11, pp. 2955–2966, Nov. 1994.

[10] I. Daubechies, *Ten Lectures on Wavelets*. Philadelphia, PA: SIAM, 1992.

[11] Ph. Delsarte, B. Macq, and D. T. M. Slock, "Signal adapted multiresolution transform for image coding," *IEEE Trans. Inform. Theory*, vol. 38, no. 2, pp. 897–904, Mar. 1992.

[12] T. Greiner, J.-P. Casel, and M. Pandit, "Texture analysis with a texture matched $M$-channel wavelet approach," in *Proc. IEEE Int. Conf. Acoust., Speech, Signal Processing*, Minneapolis, MN, vol. 5, Apr. 27–30, 1993, pp. 129–132.

[13] A. N. Iusem and A. R. De Pierro, "A simultaneous iterative method for computing projections onto polyhedra," *SIAM J. Contr. Optim.*, vol. 25, no. 1, pp. 231–243, Jan. 1987.

[14] B. Macq and J. Y. Mertés, "Optimization of linear multiresolution transforms for scene adaptive coding," *IEEE Trans. Signal Processing*, vol. 41, no. 12, pp. 3568–3572, Dec. 1993.

[15] A. Mertins, "Statistical optimization of PR-QMF filter banks and wavelets," in *Proc. IEEE Int. Conf. Acoust., Speech, Signal Processing*, Adelaide, Australia, vol. 3, Apr. 19–22, 1994, pp. 113–117.

[16] T. Q. Nguyen, "A novel spectral factorization method and its application in the design of filter banks and wavelets," in *Proc. Int. Conf. Time-Frequency Time-Scale Anal.*, Victoria, Canada, Oct. 4–6, 1992, pp. 300–306.

[17] ——, "Digital filter bank design: Quadratic-constrained formulation," *IEEE Trans. Signal Processing*, vol. 43, no. 9, pp. 2103–2108, Sept. 1995.

Authorized licensed use limited to: N.C. State University Libraries - Acquisitions & Discovery S. Downloaded on November 01,2026 at 19:48:41 UTC from IEEE Xplore. Restrictions apply.

[18] P. A. Regalia and P. Loubaton, "Rational subspace estimation using adaptive lossless filters," *IEEE Trans. Signal Processing*, vol. 40, no. 10, pp. 2392–2405, Oct. 1992.
[19] O. Rioul, "Simple regularity criteria for subdivision scheme," *SIAM J. Math. Anal.*, vol. 23, pp. 1544–1576, Nov. 1992.
[20] O. Rioul and P. Duhamel, "A Remez exchange algorithm for orthonormal wavelets," *IEEE Trans. Circuits Syst. II*, vol. 41, no. 8, pp. 550–560, Aug. 1994.
[21] M. V. Tabezay and A. N. Akansu, "Progressive optimization of time-frequency localization in subband trees," in *Proc. IEEE Time-Frequency Time-Scale Anal. Symp.*, Philadelphia, PA, USA, Oct. 25–28, 1994, pp. 128-131.
[22] A. H. Tewfik, D. Sinha, and P. Jorgensen, "On the optimal choice of a wavelet for signal representation," *IEEE Trans. Inform. Theory*, vol. 38, no. 2, pp. 747–765, Mar. 1992.
[23] M. K. Tsatsanis and G. B. Giannakis, "Principal component filter banks for optimal wavelet analysis," *IEEE Trans. Signal Processing*, vol. 43, no. 8, pp. 1766–1777, Aug. 1995.
[24] M. Unser, "An extension of the Karhunen-Loève transform to wavelets and perfect reconstruction filter banks," in *Proc. SPIE, Math. Imaging: Wavelet Applications Signal Image Processing*, San Diego, CA, vol. 2034, July 15–16, 1993, pp. 45–56.
[25] ——, "On the optimality of ideal filters for pyramid and wavelet signal approximation," *IEEE Trans. Signal Processing*, vol. 41, no. 12, pp. 3591–3596, Dec. 1993.
[26] P. P. Vaidyanathan, T. Q. Nguyen, Z. Doganata, and T. Saramaki, "Improved technique for design of perfect reconstruction FIR QMF banks with lossless polyphase matrices," *IEEE Trans. Acoust., Speech, Signal Processing*, vol. 37, no. 7, pp. 1042–1056, July 1989.
[27] P. P. Vaidyanathan, *Multirate Systems and Filter Banks*. Englewood Cliffs, NJ: Prentice-Hall, 1992.
[28] L. Vandendorpe, "CQF filter banks matched to signal statistics," *Signal Processing*, vol. 29, no. 3, pp. 237–249, Dec. 1992.

## Using the Residual Area Criterion for Signal Reconstruction from Noiseless and Noisy Samples

R. L. Kashyap and Shankar Moni

*Abstract*— **We consider reconstruction of a signal from a univariate data set. A problem that is often observed using existing techniques is overshoots between data samples. We propose a criterion, called the residual area criterion, which addresses this problem. The curve of minimum arc length that interpolates the data is the piecewise linear curve connecting the data points. Our criterion is to minimize the $\mathcal{L}^2$ distance to this curve from the chosen set of functions. We discuss the use of this criterion for both noisy and noiseless samples. The main point of our paper is that a significant improvement is realized by minimizing our criterion rather than requiring continuity of high order derivatives (which is the usual method employed for noiseless data) or minimizing curvature (which is the usual criterion for noisy data). A comparison of our method to existing methods is included.**

### I. Introduction

We consider the problem of fitting a smooth curve for a given univariate data set. This problem has a variety of applications, including probability density estimation for histogram data, estimation of spectral density, and other applications in atmospheric sciences [6].

Manuscript received July 11, 1994; revised August 17, 1995. This work was supported by the Office of Naval Research under contract ONR N00014-91-J-4126 and by the NSF under Grant CDR 8803017 to the Engineering Research Center for Intelligent Manufacturing Systems. It is based on the work presented at the Information Sciences and Systems Conference, Baltimore, MD, USA, 1995. The associate editor coordinating the review of this paper and approving it for publication was Prof. Stanley J. Reeves.

The authors are with the School of Electrical and Computer Engineering, Purdue University, West Lafayette, IN 47907 USA.

Publisher Item Identifier S 1053-587X(96)02402-4.

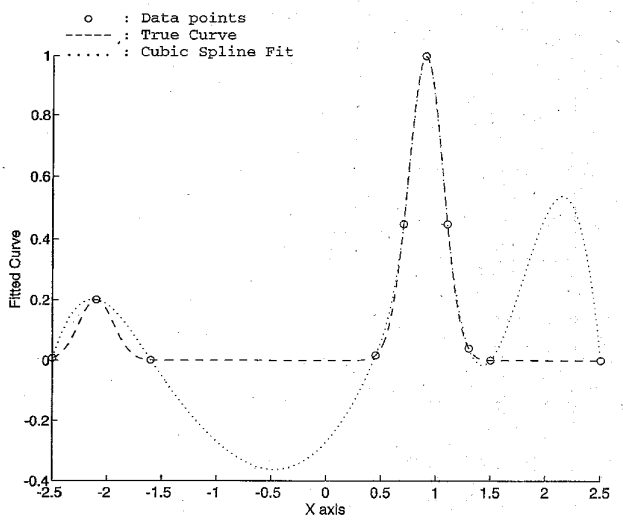



Fig. 1. Illustration of the fact that a cubic spline fit can result in large overshoots between data points. The true curve, which is a sum of two Gaussian pulses, is also shown.

Let us first consider the case of noiseless data. The most popular method for about 40 years is to fit a spline curve that passes through all data points while constraining the curve to have $M$ continuous derivatives. However, this method has a serious drawback. The fitted graph has large overshoots between successive data points as indicated in Fig. 1. If the graph is to be used to estimate a probability density function from histogram data, then large overshoots are clearly an undesirable feature. The fitted graph is not a true representation of the data since overshoots cause a significant portion of the true curve to be misrepresented.[1] Graphs fitted with the draughtsman's mechanical spline do not suffer from this drawback.

The main point of our paper is that in the context of reducing overshoots, a significant improvement is realized by minimizing our criterion rather than using conventional techniques both in the case of noiseless data [2], [5] and noisy data [6]. In order to understand this problem of overshoots a little better, let us see what would happen if we did not impose any smoothness constraint. Given data points $(x_i, y_i), i = 1, \cdots, N$, consider the graph of minimum arc length that passes through the data points. A simple variational argument shows that arc length is minimized by the piecewise linear curve connecting the data points. This curve can be written as

$$L^* = \sum_{i=1}^{N-1} L_i(x)\chi_{[x_i, x_{i+1})} \tag{1.1}$$

where $\chi_{[x_i,x_{i+1})}$ is the indicator function of the half open interval $[x_i, x_{i+1})$ and $L_i(x)$ is the line passing through the data points $(x_i, y_i)$ and $(x_{i+1}, y_{i+1})$. We would like our curve to be smooth as well as come close to $L^*(x)$. So we start with a space of smooth functions and find the function $f$ in this space that minimizes

$$J_{\text{area}}(f) = \sum_{i=1}^{N-1} \int_{x_i}^{x_{i+1}} [f(x) - L_i(x)]^2 \, dx. \tag{1.2}$$

[1] This drawback of splines was brought to our attention by Prof. Carl de Boor during his seminar at Purdue University in April 1994.

1053–587X/96$05.00 © 1996 IEEE

Authorized licensed use limited to: N.C. State University Libraries - Acquisitions & Discovery S. Downloaded on November 01,2026 at 19:48:41 UTC from IEEE Xplore. Restrictions apply.